

Research Article

Evaluation of Agrowaste Species for Removal of Heavy Metals from Synthetic Wastewater

Hussein. M. Ahmed ¹, Neama A. Sobhy ¹, Mohamed M. Hefny ²,
Fatehy M. Abdel-Haleem ³ and Mohamed A. El-Khateeb ⁴

¹Housing and Building Research Center (HBRC), Sanitary and Environmental Institute, Dokki, Giza 12613, Egypt

²Chemistry Department, Faculty of Science, Cairo University, Giza 12613, Egypt

³Cairo University Centre for Hazard Mitigation and Environmental Studies and Research CHMESR, Cairo University, Giza 12613, Egypt

⁴Water Pollution Research Department, National Research Centre, Dokki, Cairo, Egypt

Correspondence should be addressed to Mohamed A. El-Khateeb; elkhateebcairo@yahoo.com

Received 29 September 2022; Revised 17 November 2022; Accepted 20 December 2022; Published 6 February 2023

Academic Editor: Carla Patricia Silva

Copyright © 2023 Hussein. M. Ahmed et al. This is an open access article distributed under the Creative Commons Attribution License, which permits unrestricted use, distribution, and reproduction in any medium, provided the original work is properly cited.

This study's goal was to learn more about how agrowaste plants tolerate, absorb, and accumulate a number of metals that are of relevance to the environment. Adsorption of lead (Pb), chromium (Cr), selenium (Se), copper (Cu), and zinc (Zn) ions from synthetic aqueous solutions and wastewater using natural waste residues (NWRs) such as moringa, *Lupinus*, sugarcane straw, and tea residue was evaluated. The adsorbents used for this study were prepared by washing, drying, and grinding. Fourier-transform infrared (FT-IR) spectroscopy and scanning electron microscope (SEM) analysis were used to characterize the adsorbents' waste residues. The effect of different parameters such as pH, dose of adsorbents, and the initial concentration of heavy metals, as well as the adsorption isotherm parameters were studied. Moringa, *Lupinus*, sugarcane straw, or tea residue results were found to fit the Langmuir and Freundlich adsorption isotherms. The adsorption capacity reached 14.59, 16.10, 12.73, and 15.01 mg/g, respectively. The adsorption study's overall results indicated the removal efficiency pattern as moringa > tea > *Lupinus* > sugarcane straw. At a dose of 0.5 g/L, the maximum removal percentages for lead, chromium, selenium, copper, and zinc ions were 90.2, 76.55, 70.55, 76.6, and 78.9, respectively. The materials might be regarded as efficient adsorbents for extracting the ions Pb, Cr, Se, Cu, and Zn from wastewater, according to the research.

1. Introduction

Water is essential for all living creatures, for consumption, personal hygiene, irrigation, farming, the industrial sector, and many other sectors. Water resources and the environment are at risk when wastewater that has not been fully or even partially treated is discharged [1, 2]. It is extremely important to maintain the water quality standards set by applicable regulations and to eliminate hazardous substances from wastewater before discharging into the ecosystem [3, 4]. Worldwide, there is still a lot of concern about the pollution of water caused by the discharge of heavy metals. Consequently, the treatment of polluted wastewater

remains a topic of global crisis, since wastewater collected from municipalities, communities, and industries must ultimately be returned to receiving waters or to the land. Heavy metal pollution occurs in industrial wastewater such as that produced by metal plating facilities, mining operations, battery manufacturing processes, the production of paints and pigments, and the ceramic and glass industries [5].

Wastewater contamination is an ever-increasing problem that the whole world is now facing. Wastewater comprises liquid waste discharged by domestic residents, commercial properties, industry, and agriculture. Heavy metals are produced and dumped in the environment as

a result of industrialization and globalization. Unavoidably, the enormous rise in the usage of heavy metals over the past few decades has led to an increase in the flux of metallic compounds in the aquatic environment. Heavy metals are major pollutants in marine, ground, industrial, and even treated wastewater [6].

Heavy metal soil contamination is one of the most significant problems facing modern society. Heavy metals found in drinking water, surface water, groundwater, and animal tissue have exposed a vast number of individuals to health risks. Heavy metal pollution is a serious environmental problem since heavy metals are poisonous and cannot biodegrade, exacerbating their harmful effects. Some of these heavy metals are also known to attack the active sites of enzymes in the body, therefore, inhibiting the enzymes [6, 7]. Heavy metals contaminated wastewater commonly include Cd, Pb, Cu, Zn, Ni, and Cr. Whenever toxic heavy metals are exposed to the natural ecosystem, the accumulation of metal ions in human bodies will occur through either direct intake or food chains. Therefore, heavy metals should be prevented from reaching the natural environment [6, 8]. The extreme focus must be placed on heavy metal removal from wastewater [4, 5]. The long-term accumulation potential of heavy metals makes them highly harmful to humans and the human food chain. Lead, zinc, copper, chromium, selenium, and other heavy metals, for instance, have an adverse effect on environmental sources [9, 10]. Aquatic bodies are being overwhelmed with microbes and waste matter. Heavy metals enter our bodies through eating, drinking, skin, and inhaling; once in the body, these metals have serious consequences on humans such as nervous system deterioration, reproductive failures, brain damage, irritability, kidney damage, anemia, tumor formation, and muscle weakness [11]. Pollution of copper Cu^{2+} is caused by mining activities, electroplating, smelting, and the utilization of copper-based agrichemicals and manufacturing of brass. There is some uncertainty regarding the long-term effects of copper on sensitive populations such as carriers of the gene for Wilson disease and other metabolic disorders of copper homeostasis [12]. Industrial effluent containing significant zinc concentrations may cause zinc-contaminated sludge to collect on the containers [13]. In addition, a small amount of zinc taken by a person may result in a lack of appetite, a diminished sense of taste and smell, sluggish wound healing, and skin ulcers [14]. The World Health Organization (WHO) estimates the maximum permitted concentrations of Cu, Pb, Se, Zn, and Cr in drinking water to be less than 2 mg/L, 0.01 mg/L, 0.001 mg/L, 2.0 mg/L, and 0.02 mg/L, respectively. Lead in water arises from a number of industrial and mining sources and is the most widely distributed of all toxic metals. Lead in water causes serious problems such as anemia, and kidney disease and affects the nervous system [15, 16]. The Earth's crust contains a lot of chromium, which is used to plate metals. In general, food appears to be the primary source of chromium intake and on the basis of guideline values, there are no adequate toxicity studies available to provide long-term carcinogenicity studies. The effects of selenium on the environment, dietary intakes, metabolism and health, bodily processes, thyroid

hormone metabolism, antioxidant defense mechanisms, oxidative metabolism, and the immune system are extensive [17].

In addition to industrial byproducts and natural materials, agricultural waste is one of the abundant sources of low-cost adsorbents that is gaining scientific interest [18–22]. Agricultural waste, such as wheat bran, rice husk, peanut husk, and sawdust, is widely available but has little commercial value. It also poses significant disposal challenges [6]. Many such materials have been investigated, including microbial biomass, peat, compost, leaf mold, palm press fibers, coal, sugarcane bagasse, straw, corncob [23], wool fibers, and byproducts of rice mill, soybean, and cottonseed hulls, tea waste, leaf powder, pomegranate peel, olive bagasse, and hazelnut. The agricultural residues or industrial by-products having biological activities have been received with considerable attention. The effectiveness of rice straw, sugarcane bagasse, soybean, and cottonseed byproducts as metal ion adsorbents in an aqueous solution was examined. Agricultural by-products and biological materials have been found to be useful for metal sorption. These wastes are considered to be good metal scavengers from solution and wastewater as they contain certain functional groups [6, 7]. The objective of this study is to produce materials that are beneficial for removing heavy metals while also valorizing agricultural waste. The removal of heavy metals from tea waste residue, *Lupinus*, moringa, and sugarcane straw was investigated. The behavior of metal ions adsorption onto the studied bio-adsorbent as affected by pH, dosage, contact time, and initial concentration was studied. The work was extended to study the isotherm and kinetic parameters for the adsorption processes.

2. Experimental Setup

2.1. Instruments and Characterization Techniques. The muffle (Thermo Fisher, American provider of scientific instruments) was used in this study. The content of heavy metals was measured using an atomic absorption spectrometer (AAS) fitted with a graphite furnace (ICE 3000 AAS from American scientific equipment manufacturer Thermo Fisher). Also, a flame atomic absorption spectrometer (FAAS), equipped with a deuterium lamp for background correction, a single-element hollow cathode lamps, and air-acetylene burner was used for the determination of Pb, Zn, Se, Cu, and Cr ions, at their respective wavelengths 217.0 nm, 330.4 nm, 260.4 nm, 327.4 nm, and 357.9 nm.

All of the samples were cleaned with distilled water (DW) (Millipore GER), dried in an oven (Fisher Scientific Equipment, American-made scientific equipment) and then allowed to dry for 24 hours at that temperature. Digital electronic balance (PCE Instruments UK) was used, and the pH measurements of the samples were achieved using a pH meter (AD110, Adwa, Hungary). Thermo Fisher Scientific (UK) equipment was used to record the spectra of adsorbents both before and after treatment using Fourier-transform infrared spectroscopy (FT-IR) analysis. An FT-IR infrared spectrometer was used to identify the functional

groups present in the adsorbents. Adsorbents samples were proportionally macerated with KBr crystals (1 mg sample/100 mg KBr) and put in a pastillator, then 4,000 to 400 cm^{-1} spectral range was analyzed. Shaking was performed by using a programmable shaker system (USA). Surface images of adsorbents were recorded using Quanta FEG 250 scanning electron microscope (FEI Company, USA). Samples were mounted onto SEM stubs. The following SEM settings were used: 10.1 mm working distance, and 20 kV excitation voltages for the in-lens detector.

2.2. Preparation of Adsorbents. The used solutions have also been prepared using distilled water. All glassware has been carefully cleaned using multiple washings. Analytical grade chemical reagents were used throughout the experiment. Tea waste residue (TWR) was produced from waste and washed with boiled water until the water was colorless. This process was repeated and after that, it keeps in a drier at 105°C for 12 h to remove the moisture content. The dried substances were changed into powder and screened the sizes up to 100 μm . Again, the powder dried at 105°C for 5 h, now the adsorbent is ready to use [24]. Egypt, a country that produces lupines, was the subject of the research. It was dried at 105°C overnight to remove the moisture contents, ground, and sieved (sieve, 90 μm) to obtain a more homogeneous particle size. Next, the material was dried at 105°C for 12 h to obtain a finer particle size. Sugarcane straw produced by the juice shops, in Giza, Egypt, was used for the experiments. It was ground and sieved (sieve, 90 μm) to obtain a more homogeneous particle size. Next, the material was dried at 105°C for 12 h to remove the moisture content. Moringa used in the experiment was obtained from NRC, Egypt. It was ground and sieved (sieve, 90 μm) to obtain a more homogeneous particle size. Next, the material was dried at 105°C for 12 h to remove the moisture content. In order to use the moringa, it was immersed in distilled water for 24 hours to remove any remaining oil after the mechanical press. Then, the moringa was then filtered and dried at 105°C. The seeds of moringa were prepared by taking of the seed powder and mixing it with water. The moringa seeds were poured into the water samples that were to be purified. The samples were examined using the AAS after standing for between 15 and 120 minutes in all tests, which were carried out at room temperature. Figure 1 summarized the preparation of the adsorbents from the different natural waste residues (NWRs). According to Figure 2, all adsorbents were ready for usage.

2.3. Preparation of Adsorbate. Synthesized heavy metals were prepared from stock solutions of 1000 mg/L Cu, Pb, Se, Zn, and Cr ions dissolved in HNO_3 . The required dilutions were carried out with deionized water using the 0.1 M sodium hydroxide (NaOH) and hydrochloric acid (HCl) solution.

2.4. Analysis. The concentrations of heavy metals in the solutions before and after equilibrium were determined by using an atomic absorption spectrometer. The pH of the

solution was measured with a Hanna pH meter using a combined glass electrode. A wrist motion shaker was used to do the shaking. Deionized and double-distilled water were used for the jar test. Each analysis was completed in accordance with APHA guidelines [25].

2.5. Contact Time's Impact on the Adsorption Profile. The adsorption experiments were performed with each material and ion, separately, using 1 L of solutions. In an orbital shaker, the initial concentration of 3.0 mg/L was stirred with 0.1 g of adsorbents. The samples were taken from the supernatant between the times of 15 and 120 minutes. The concentration of metals ion in each aliquot was determined by AAS.

2.6. Adsorbent Dose's Impact on the Adsorption Profile. Batch studies also include the examination of the impact of adsorbent dose on the adsorption capacity of the adsorbents [26]. The adsorbent was mixed with a synthesized aqueous solution at various dosages (0.1, 0.2, 0.3, 0.4, and 0.5) g/L in the combined system. The synthesized aqueous solution volume used in the experiment was 1 L.

2.7. Effect of Initial Concentration. The effect of an initial concentration of heavy metals on the adsorption efficiency of adsorbents is determined in this experiment. It was performed by preparing different concentrations of heavy metals. The Cu, Pb, Se, Zn, and Cr ion solutions were agitated at 100 rpm, and the temperature was kept constant at $25 \pm 1^\circ\text{C}$. The adsorbent was mixed with a synthetic aqueous solution at concentrations of 0.5, 1.0, 2.0, 3.0, 5.0, and 10 mg/L at a constant contact time of 90 min and a dose of 0.1 g. The volume of the synthetic aqueous solution was 1 L.

2.8. Effect of pH. Among the many variables that affect the metal adsorption process is the pH. The pH is the most critical parameter affecting any adsorption studies due to their interference in the solid-solution interface, affecting the charges of the active sites of the adsorbents and the metal behavior in the solution [27]. The influence of pH on the adsorption of Cu, Pb, Se, Zn, and Cr ions in the solution has been demonstrated, and it is now recognised as a key factor influencing the process' effectiveness. Cu, Pb, Se, Zn, and Cr ions were removed from the aqueous solution at different pH levels (3–9) using a constant dosage of 0.1 g/L at 100 rpm/90 min.

2.9. Batch Studies Using Adsorbent. The adsorption isotherms were comprehensively investigated. The effect of operating parameters on the adsorption efficiency was examined. The effect of the dose of adsorbent, and concentration of metals on removal efficiency (%), and capacity q_{max} (mg/g) of metals were characterized [28]. The removal efficiency ($R\%$), the dose of metals adsorbed on a specific dose of adsorbent q_e (mg/g) were calculated from the following equations:

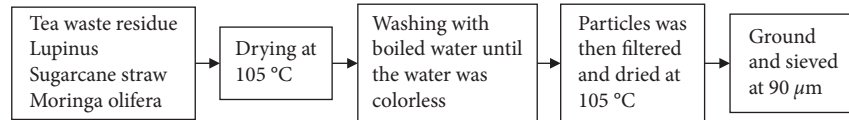


FIGURE 1: Flow chart illustrating the creation of adsorbents from natural waste residues (NWRs).



FIGURE 2: The images of the prepared adsorbents, lupines, sugarcane straw, tea, moringa seed, and moringa leaves.

$$R\% = \frac{C_o - C_e}{C_o} \times 100, \quad (1)$$

$$q_e \left(\frac{mg}{g} \right) = \frac{(C_o - C_e)V}{m},$$

where $R\%$ is the removal efficiency, q_e is the dose of metals adsorbed on a specific dose of adsorbent (mg/g), C_o is the initial concentration (mg/L), C_e is the concentration after adsorption (mg/L), m is the dose of adsorbents (g), and V is the volume of solution (Liter).

2.9.1. Langmuir Isotherm Model. Adsorption isotherms, which are typically the ratio between the amount adsorbed and that was left in solution at equilibrium at a specific temperature, were used to describe equilibrium studies [29]. The Langmuir model is predicated on the hypothesis that maximal adsorption happens in the presence of a saturated monolayer of solute molecules on the adsorbent surface, the adsorption energy is constant, and there is no adsorbate molecule migration in the surface plane. According to the Langmuir equation, monolayer sorption is caused by

physical causes. You may find the Langmuir isotherm equation by using

$$q_e = \frac{C.K q_{\max}}{1 + KL},$$

$$\frac{C_e}{q_e} = \frac{1}{q_{\max} \cdot KL} + \frac{C_e}{q_{\max}}, \quad (2)$$

$$RL = \frac{1}{1 + C_o.KL},$$

where q_{\max} and K are the Langmuir constants, q_e is the dose of metals adsorbed on a specific dose of adsorbent (mg/g), C_e is the equilibrium concentration of the solution (mg/L), and q_{\max} is the maximum dose of metals concentration required to form a monolayer (mg/g). The values of q_m and K can be determined from the linear plot of C_e/q_e versus C_e [30].

2.9.2. Freundlich Isotherm Model. The Freundlich isotherm model that many sites with various adsorption energies was involved in the empirical relationship that describes the

adsorption of dissolved solutes to a solid surface. The characteristics of the system are K_F and n are the indicators of the adsorption capacity and adsorption intensity, respectively. The Freundlich model's capacity to match the experimental data was investigated. The intercept value of K_F and the slope of n were calculated for this scenario using the plot of $\log C_e$ vs. $\log q_e$. The Freundlich isotherms appear when the surface is heterogeneous and the absorption is multilayered and bound to sites on the surface.

$$\log q_e = \log KF + \frac{1}{n} \log C_e, \quad (3)$$

where K is the Freundlich equilibrium constant (mg/g), $1/n$ = intensity parameter, C_e = equilibrium concentration of adsorbate, and q_e is the dose of solute adsorbed [31–33]. The Freundlich model with linear plotted $\log q_e$ versus $\log C_e$ is shown in equation (3) [16].

The constants K_f and $1/n$ are produced via the Freundlich formulation in a linear form. Freundlich isotherm model assumes nonideal adsorption on heterogeneous surfaces in a multilayer coverage. It suggests that stronger binding sites are occupied first, followed by weaker binding sites. In other words, as the degree of site occupation increases, the binding strength decreases.

2.10. Kinetic Study. It was possible to characterize the kinetics for each adsorbent, using pseudo-first- and pseudo-second-order kinetic models. The pseudo-first-order kinetics follows the Lagergren model expressed by

$$\text{Log}(q_{eq} - q_t) = \log q_{eq} - K_1 \cdot \frac{t}{2.303}, \quad (4)$$

where q_t is the adsorbed dose of metallic ions (mg/g) in t time (min) and k_1 is the pseudo-first-order constant (min^{-1}). Through linear and angular constant of log graphic ($q_{eq} - q_t$) in the function of time, q_{eq} and k_1 can be calculated, respectively. Comparing the values for q_{eq} derived by equation (5) and those observed experimentally:

$$\frac{t}{qt} = \frac{1}{K_2 q_{eq}^2} + \frac{t}{q_{eq}}, \quad (5)$$

where k_2 is the pseudo-second-order constant ($g/mg \cdot \text{min}$) obtained by calculation of linear coefficient and q_{eq} is calculated through angular coefficient.

3. Results

3.1. Characteristics of Adsorbents. Scanning electron microscopy (SEM) was used to characterize the surface morphology of adsorbents (Figures 3(a)–3(e)). The FT-IR of adsorbents before adsorption is shown in Figures 3(a)–3(e). The micrographs, Figures 2(a)–2(e), show the porous structures and the pore sizes of different adsorbents. These surface characteristics will lead to enhanced metal binding because the metal ions have access to binding cavities [34].

Investigating the functional groups of natural waste materials as adsorbent that is responsible for the adsorption of metals, Fourier-transform infrared (FT-IR) spectrum

analysis was performed. Figures 4(a)–4(e) illustrate FT-IR spectra of adsorbents before adsorption. The FT-IR spectrum of adsorbents was found to be in the $1000\text{--}4000\text{ cm}^{-1}$ range. There are peaks, with a strong band of amine or hydroxyl (N-H or -OH) groups at wave number 3400 [35]. The metal ion-binding mechanism of adsorption is attributed to the abundance of hydroxyl groups from cellulose, in which an aqueous medium favors ion exchange or complexation with metal ions [36]. The band presented at 2923 cm^{-1} may indicate the -C-H stretching vibration from aliphatic compounds. The adsorbent's N-H bending was demonstrated by the absorption at, 1597 cm^{-1} . At wave number 1437 cm^{-1} , the C=N stretching in heterocyclic rings was also discovered. The peak at 1316 cm^{-1} is attributed to the C-OH stretching vibration of alcohols. Finally, the carboxylic acids were observed at, 1156 cm^{-1} of the adsorbents [22]. The carboxylic groups present in adsorbents are usually weak acids and make negative sites in medium and moderately acid [27]. These groups are usually weak acids that depending on the pH become negative sites that facilitate cation interaction in solution. Typically, pH is the appropriate level for these sites to become more reactive ($5.0\text{--}6.0$) [18]. The metal ion-binding capacity of adsorbents can be intensified by the introduction of surface groups with capacity chelating as carboxylate or amine. The introduction of carboxylic functions (-COOH) on cellulosic fiber, lignin, and hemicellulose can be performed via cyclic anhydride reaction [27]. The bio-sorption of metal by adsorbents is attributed to the availability of carboxyl groups, especially of amino acids' functionality interacting with metals ions to form ligands Cu, Pb, Cr, Zn, and Se are the most significant contaminants [27]. By comparing the removal of the metal ions Cu, Pb, Cr, Zn, and Se, it can be seen that the functional groups in the adsorbents are nearly identical. Nevertheless, some little differences have been observed on metal peaks of 1604 cm^{-1} and 1156 cm^{-1} found in Cu, Pb, Cr, Zn, and Se removal. This resulted from interactions between the carboxylic acid groups and the carbon aromatic structures of metals, respectively, on the surface of adsorbents. The adsorption of both Cu and Se ions from wastewater is greatly aided by the presence of carboxylic acids, amines, alcoholic aldehydes, and amide groups in adsorbents. These results showed also that adsorbents can remove Cu, Pb, Cr, Zn, and Se by both textural properties (microporosity and surface area) and their heterogeneous functional groups [37].

3.2. Contact Time's Impact. The time needed for metal ion biosorption is highly dependent on the specific kind of biosorbent. Batch biosorption tests were conducted under ideal conditions at intervals ranging from 15 to 120 minutes to determine the impact of contact time on biosorption. Figures 5(a)–5(e) demonstrate that Pb, Cu, Cr, Se, and Zn exclusion increased within the first 15 minutes of contact time, and that equilibrium was reached for all biosorption within 90 minutes, as no additional rise in metal ion removal could be observed after 120 minutes.

The highest adsorption was observed for the Pb, followed by Cu, Cr, Se, and Zn. The system tended to attain

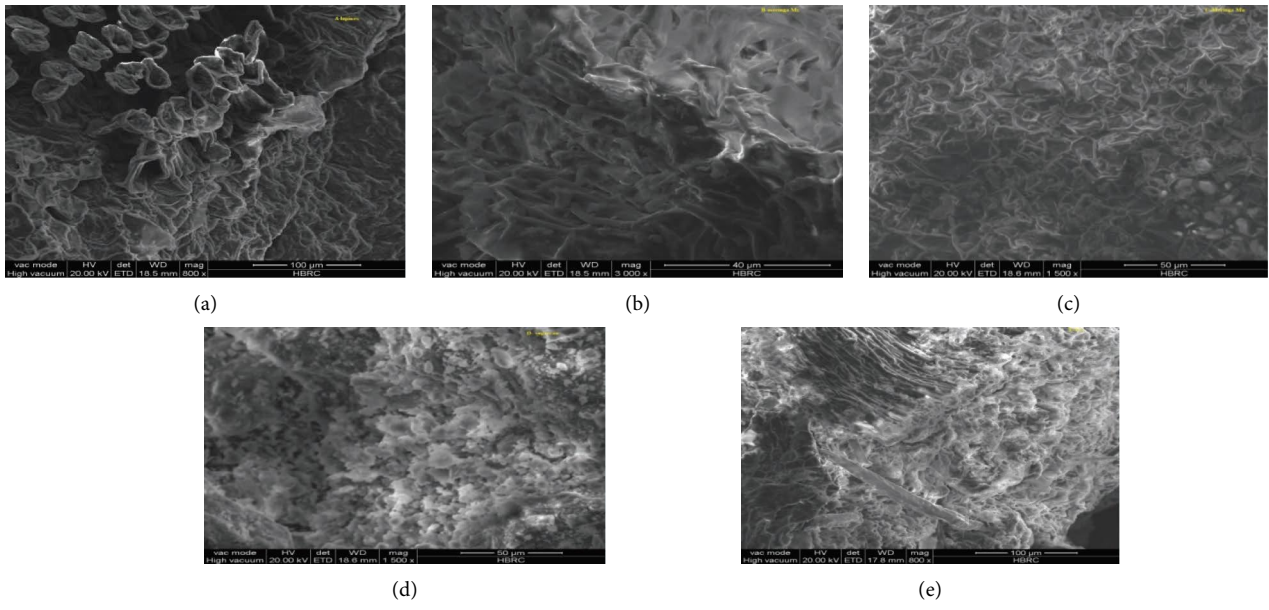


FIGURE 3: (a–e) The SEM images of the surface adsorbents: (a) moringa seed, (b) moringa leaves, (c) tea, (d) lupines, and (e) sugarcane straw.

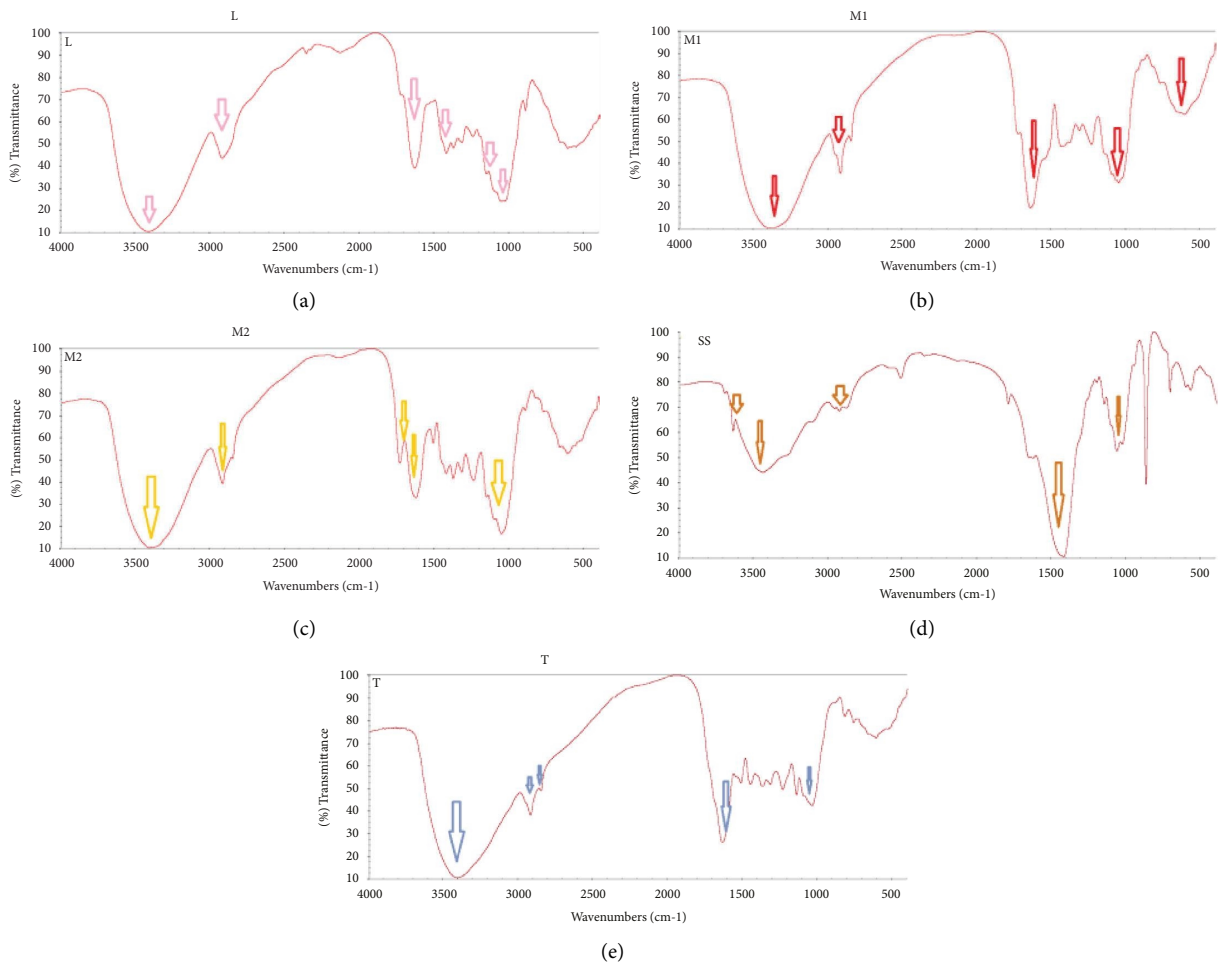


FIGURE 4: (a–e) The FT-IR spectrum of all adsorbents: (a) lupines, (b) moringa leaves, (c) moringa seed, (d) sugarcane straw, and (e) tea.

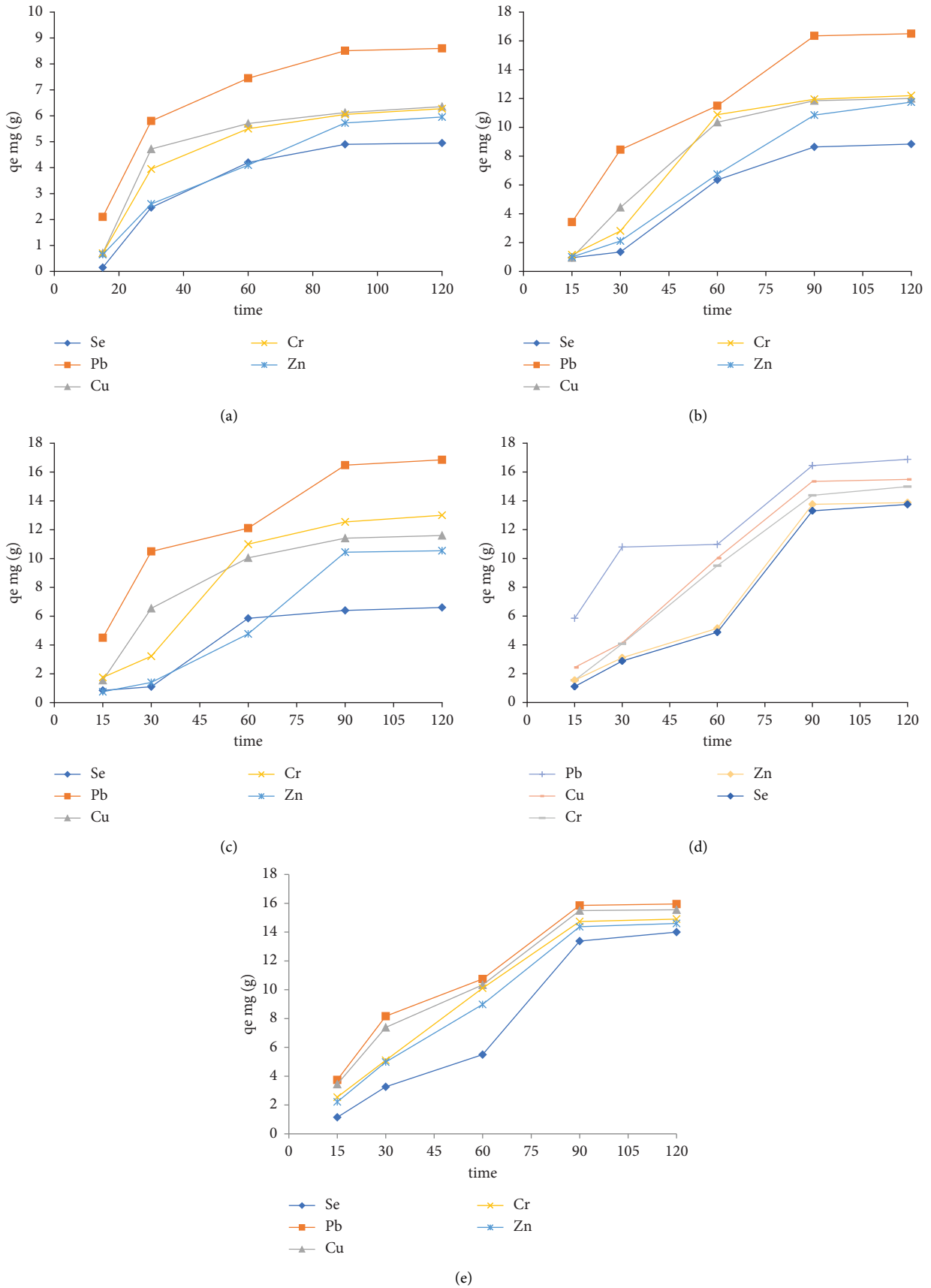


FIGURE 5: (a–e) The relationship between the amount of metal adsorbed (mg/g) and time (15, 30, 60, 90, and 120) min using an aqueous solution of Cu, Pb, Se, Zn, and Cr (pH 6.0, dosage 0.1 g 100 rpm/30 min, and 2.0 mg/L). (a) Adsorption of moringa L. (b) Adsorption of moringa B. (c) Adsorption of tea. (d) Adsorption of lupinus. (e) Adsorption of sugarcane straw.

equilibrium for all studies at around 90 minutes; nevertheless, a modest increase in adsorption was confirmed at about 120 minutes. Dos Santos et al. reached equilibrium after around 90 minutes [38]. Ghorbel-Abid and Trabelsi-Ayadi obtained system equilibrium in around 120 min [39]. It is evident from Figures 4(a)–4(e) that the bio-sorption process comprised of two steps; the first one was the fast step which lasted for a shorter time and was preceded by a second phase which was slower and lasted until the attainment of equilibrium. It has been noted that there were initially a lot of open sites that could be acquired for bio-sorption; as a result, metal ions occupied these sites during the first stage. After time has passed, the leftover vacant sites are hard to be occupied because of repulsive forces among the adsorbate molecules on the bio-sorbent surface and those present in the bulk liquid phase.

3.3. Adsorbent Dosage Effect. The effect of the adsorbent dose was studied at room temperature (25°C) by varying the sorbent doses from 0.1 to 0.5 g/L. Heavy metal contents were set at 2.0 mg/L from the beginning. The adsorption of Cu, Pb, Se, Zn, and Cr is shown in Figures 6(a)–6(e), and it increased quickly with the dose of adsorbents due to higher surface area availability at a higher concentration of the adsorbent. The significant increase in uptake was observed when the dose was increased from 0.1 to 0.4 g/L. Beyond this point, adding more adsorbent had no discernible impact on the adsorption. The overlap of adsorbent sites as a result of adsorbent particle crowding may be the cause of this. The percentage of metal adsorption on adsorbents is found to depend on the sorption capacity of the adsorbents within a range of starting metal concentration [10, 24].

3.4. Effect of Initial Concentration. The effect of the initial concentration on the Cu, Pb, Se, Zn, and Cr removal efficiencies at a constant dose of 0.1 g/L is observed in Figures 6(a)–6(e), the Cu, Pb, Se, Zn, and Cr removal percentages were greater at lower initial metal concentrations in the solutions [22]. The studies are carried out at various adsorption process concentrations for Cu, Pb, Se, Zn, and Cr (0.5, 1.0, 2.0, 3.0, 5.0, and 10 mg/L). The results revealed that the removal efficiencies were decreased with increasing Cu, Pb, Se, Zn, and Cr ion concentrations, as observed in Figures 7(a)–7(e). This has happened because Cu, Pb, Se, Zn, and Cr ions have quickly adhered to the adsorbent sites. This means that the removal efficiencies were lower at the higher initial concentration values. Here, the removal efficiencies of Cu, Pb, Se, Zn, and Cr ions in this process decreased as increasing the concentration from 0.5 to 10 mg/L in the first 30 min as shown in Figures 7(a)–7(e) [10].

3.5. pH's Impact on the Adsorption Process. The pH dependence of metal ions' uptake was linked to both the surface functional groups and the metal ion species predominant in an aqueous solution. The species metals (M)

and M(OH) are predominant at pH lower than 6, while the groups on the surface are protonated and cannot bind to metal ions in the solution. Besides, at very low pH, the surface groups are associated with the hydronium ions (H_3O^+), negatively affecting the interaction with the metal cations. When the pH increases, the surface affinity with the metal also increases, and adsorption is improved [40]. One of the essential factors for the sequestration of heavy metal ions by adsorption from aqueous solutions is the initial solution pH. It influences the charge on the adsorbent surface, the degree of ionization, and the species of adsorbates [41]. The effect of pH on the elimination of Cu, Pb, Se, Zn, and Cr ions from aqueous solution at constant initial concentration was examined in the current research effort at pHs of 3, 6, and 9. The Cu, Pb, Se, Zn, and Cr ions removal percentage was significantly higher at pH 6 than at lower pH values for all five forms of adsorbents as shown in Figures 8(a)–8(e). The presence of more vacant sites for the bio-sorption of Cu, Pb, Se, Zn, and Cr ions in the acidic medium may be the cause of higher adsorption at pH 6.0. In addition, at the ideal pH, there were more negatively charged functional groups available on the biosorbent's surface for binding Cu, Pb, Se, Zn, and Cr ions. This resulted in a decreased struggle between protons and metal ions [10, 41, 42]. The percentage of Cu, Pb, Se, Zn, and Cr ion removal was a law at pH 3.0 and 9.0 during the adsorption process because the solution was acidic [9, 10], high alkaline, but at pH 6.0, the removal efficiency was very high [4, 9]. The removal efficiency of Cu, Pb, Se, Zn, and Cr ion for the case of adsorbents reached 82.2%, 93%, 81.55%, 82%, and 82% at pH = 6.0 [36], respectively. Similar results were found by Homagai et al. [43].

3.6. Adsorption Isotherms. The adsorption isotherms of the studied metals on the moringa (leaves and branch), tea, lupines, and sugarcane straw, were based on the optimum operating conditions which were 0.10 g at pH 6.0 (Figures 9(a)–9(e)). According to the Langmuir and Freundlich mathematical models, the linearization was carried out. The computed parameters for the Langmuir and Freundlich models are shown in Table 1, along with the correlation coefficients for the adsorption data. The experimental results of Cu, Pb, Cr, Zn, and Se adsorption on the moringa (L, and B), tea, lupines, and sugarcane straw were similar in both the models used since the difference between R^2 was negligible [44]. The model that good fitted for metal adsorption was Freundlich, indicating that the adsorption occurred in multiple layers. Linearization data showed the best fit by the Langmuir model for metal, which shows higher monolayer adsorption [44].

In the Langmuir linearization, it was verified that Pb had a higher adsorption efficiency (q_m) compared to Cu, Cr, Se, and Zn; however, comparing the parameter " K_L ," Pb showed the highest binding energy with the adsorbent ($K_L = 19$).

The values of K_f were determined from Figures 9(a)–9(e) for Cu, Se, Zn, Pb, and Cr as the adsorbents ranged

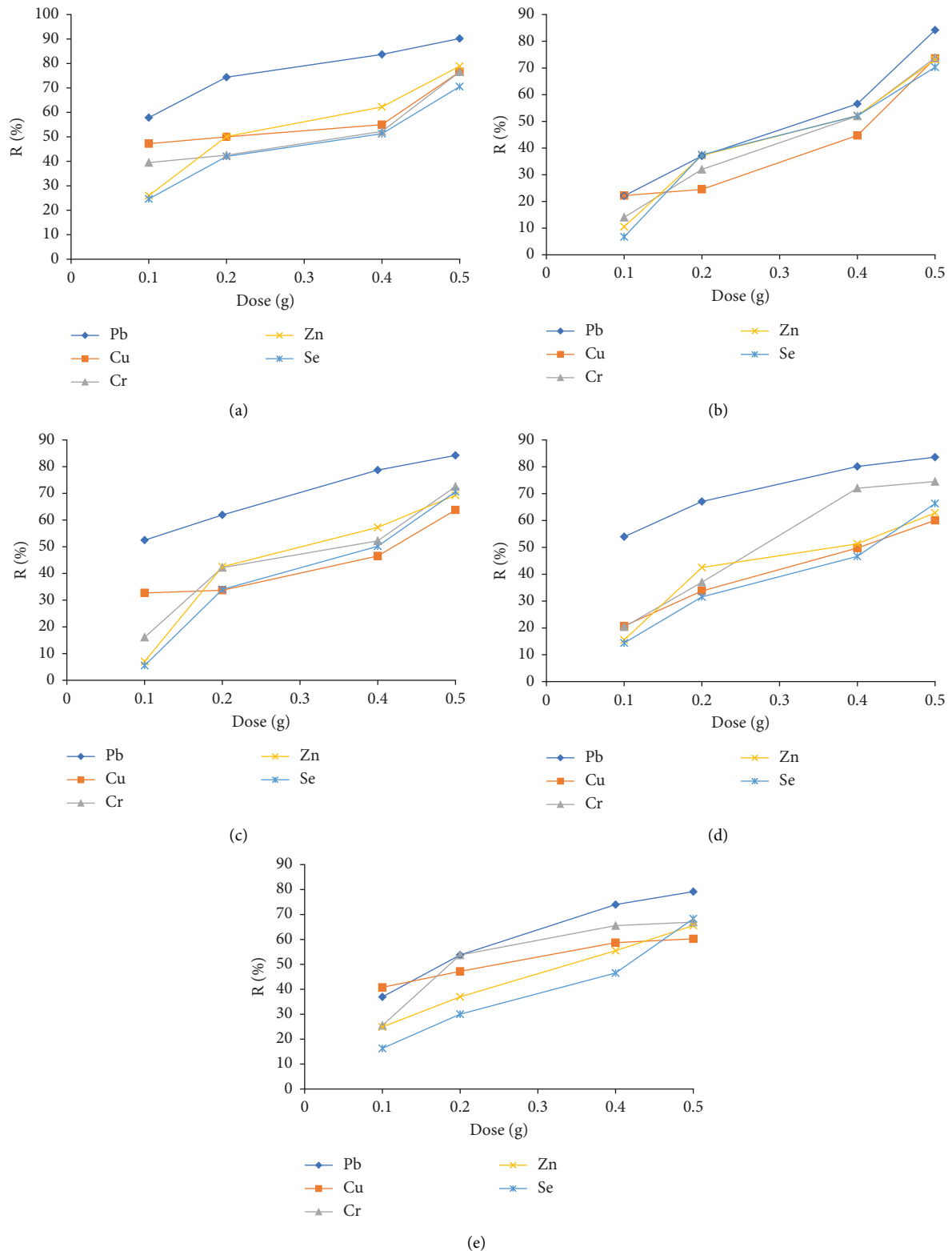


FIGURE 6: (a-e) The relation between removal efficiency (%) of adsorbents and dose (0.1, 0.2, 0.4, and 0.5) (g), the aqueous solution containing Cu, Pb, Se, Zn, and Cr, time 30 min, 100 rpm, concentration 2.0 mg/L, and pH 6.0. (a) Adsorption of metals on ML. (b) Adsorption of metals on MB. (c) Adsorption of metals on T. (d) Adsorption of metals on L. (e) Adsorption of metals on S.

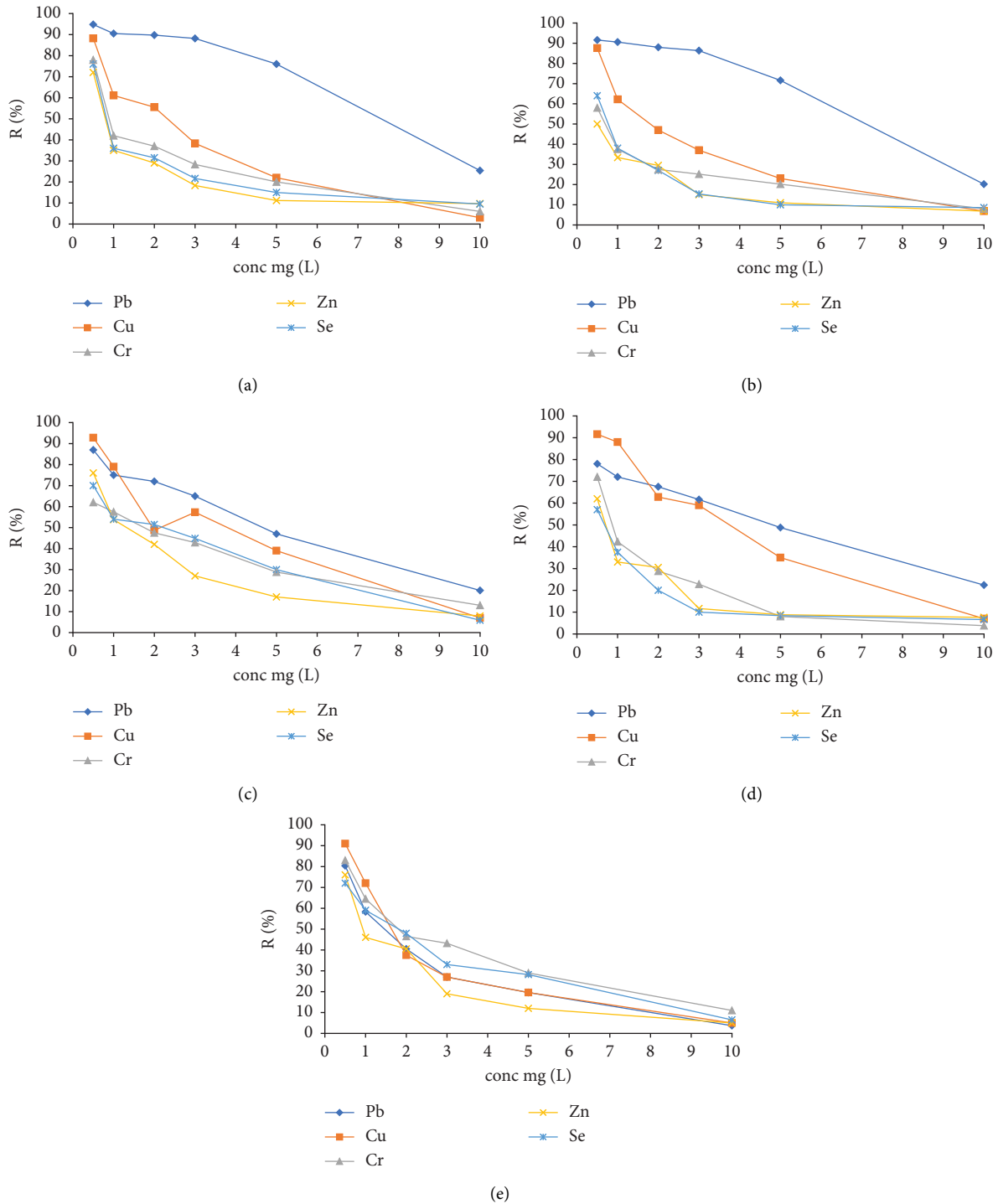


FIGURE 7: (a–e) Relation between removal efficiency (%) and initial concentration (0.5, 1.0, 2.0, 3.0, 5.0, and 10.0) (mg/L), the aqueous solution containing Cu, Pb, Se, Zn, and Cr, time 30 min, 100 rpm, dose 0.1 g, and pH 6.0. (a) Adsorption of metals on ML. (b) Adsorption of metals on MB. (c) Adsorption of metals on T. (d) Adsorption of metals on L. (e) Adsorption of metals on S.

from 1.8 to 12.5 (mg/g). This adsorption sequence can be associated with the characteristic of each metal and the form of interaction with the adsorbent, and n is >2.0 . The magnitudes of K_F and n show the easy separation of metal ions from the aqueous solution and indicate favorable adsorption [22, 24, 44]. It was observed that Pb ion was preferentially

adsorbed over other metal species, as indicated in Figures 9(a)–9(e)). This fact may be related to its higher positive charge and ease to form hydrolyzed species, which has a significant effect on the adsorption.

The effect of isotherm shape is discussed by the direction of predicting whether an adsorption system is

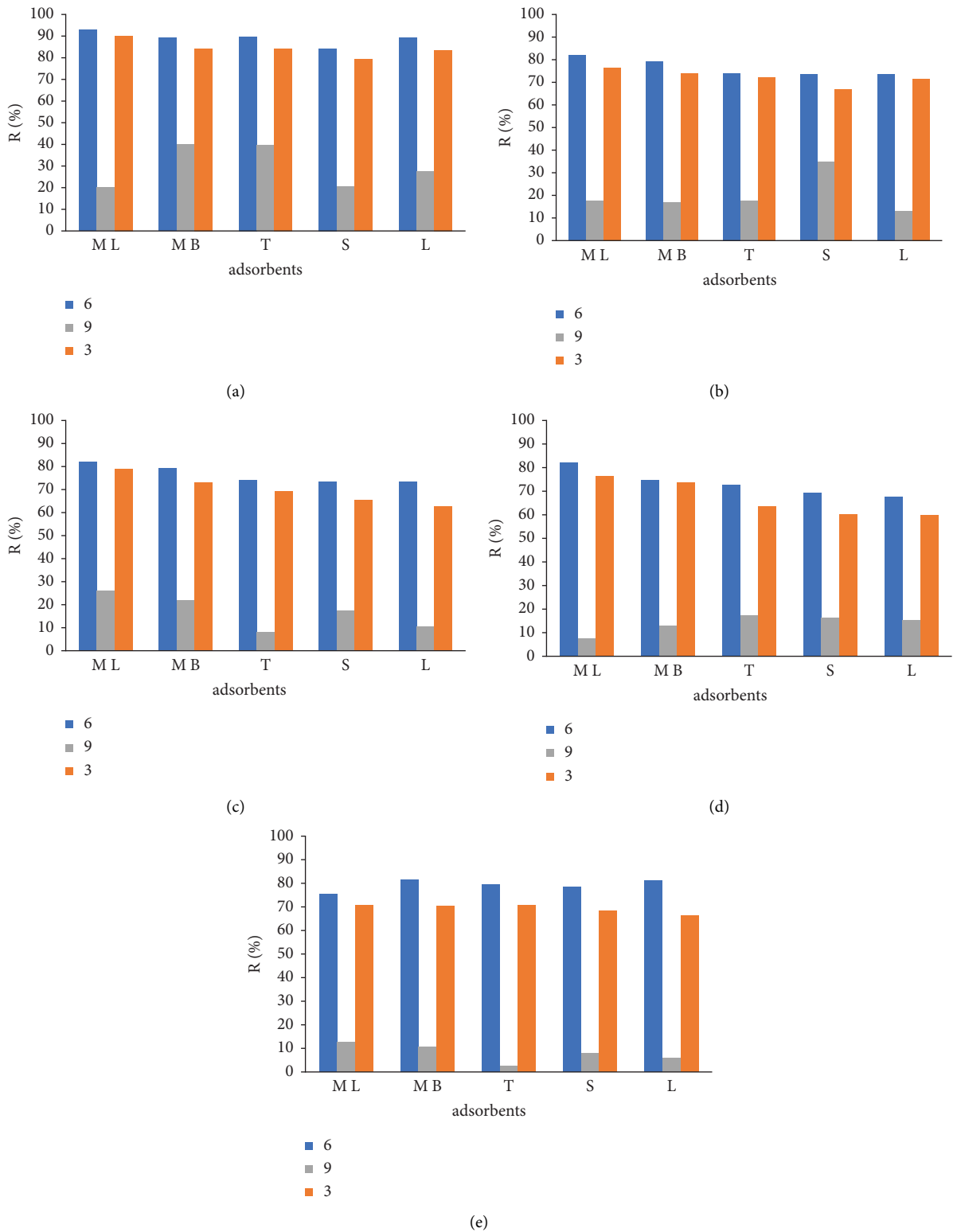
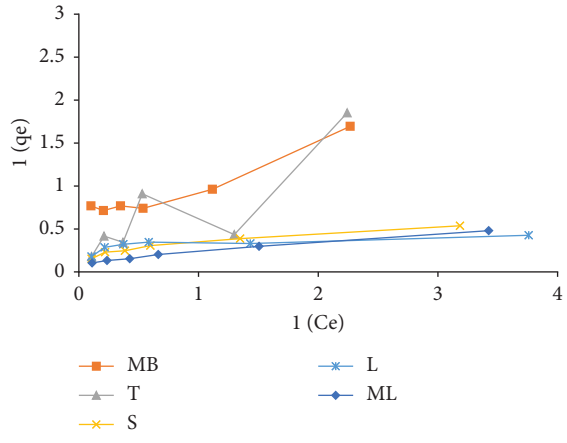
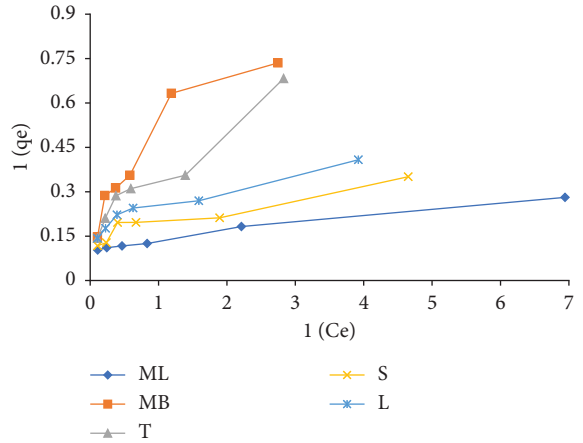


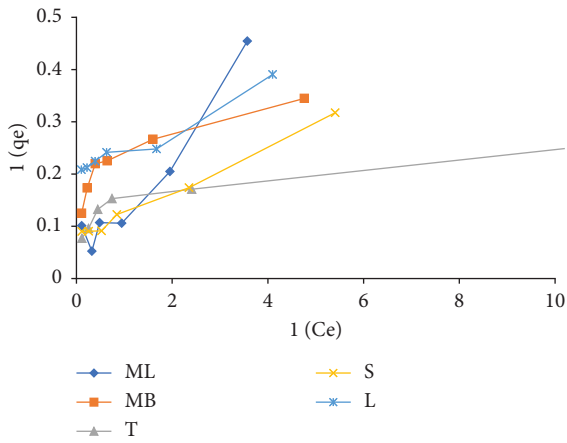
FIGURE 8: (a–e) Influence of pH on removal of Cu, Pb, Se, Zn, and Cr by adsorbents. The other conditions were kept constant during the adsorption processes. Dose = 0.1 g/L, initial conc. = 2.0 mg/L, and rpm 100/30 min. (a) Adsorption of Pb. (b) Adsorption of Cr. (c) Adsorption of Zn. (d) Adsorption of Cu. (e) Adsorption of Se.



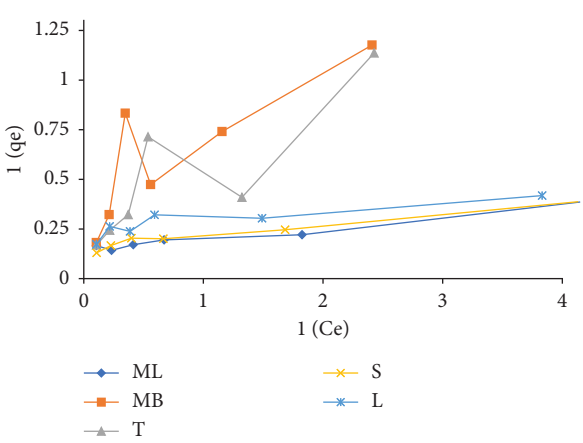
(a)



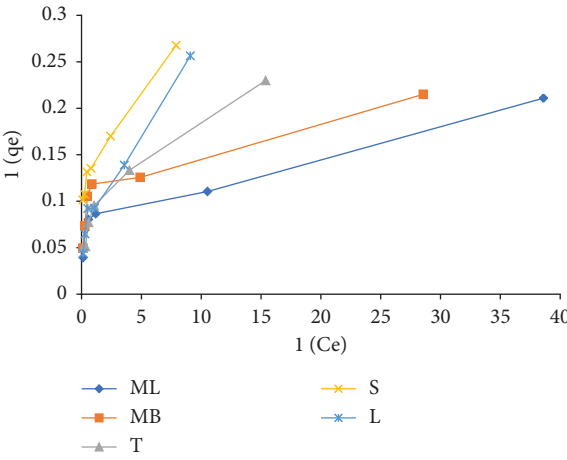
(b)



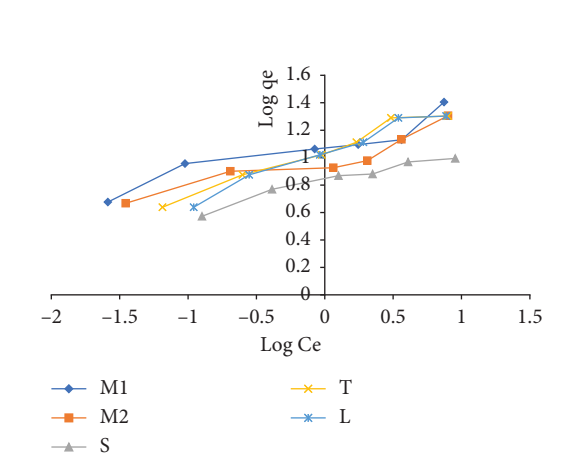
(c)



(d)



(e)



(f)

FIGURE 9: Continued.

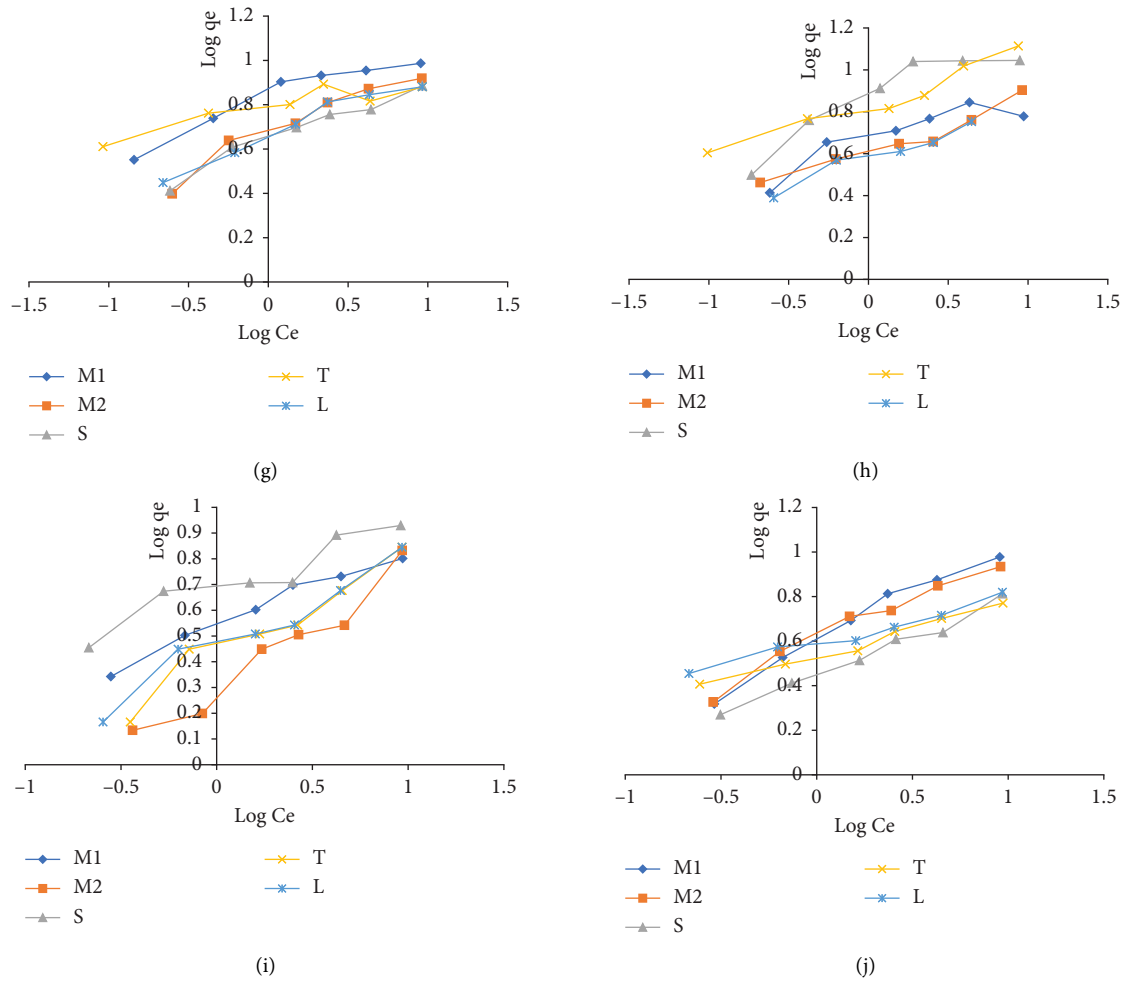


FIGURE 9: (a–j): The isotherms models (Langmuir and Freundlich) of Pb; Cr Se Cu, and Zn onto moringa (L, and B), tea, lupines, and sugarcane straw. (a) Langmuir model of Se on different adsorbents. (b) Langmuir model of Cr on different adsorbents. (c) Langmuir model of Cu on different adsorbents. (d) Langmuir model of Zn on different adsorbents. (e) Langmuir model of Pb on different adsorbents. (f) Freundlich model of Pb on different adsorbents. (g) Freundlich model of Zn on different adsorbents. (h) Freundlich model of Cr on different adsorbents. (i) Freundlich model of Cu on different adsorbents. (j) Freundlich model of Se on different adsorbents.

“favorable” or “unfavorable.” Suggested a dimensionless separation factor or equilibrium parameter, R_L , as an essential feature of the Langmuir isotherm to predict if an adsorption system is “favorable” or “unfavorable. Table 1 presented that the correlation coefficient (R^2) of Langmuir is slightly higher than that of Freundlich adsorption isotherm. Here, C_0 = reference fluid-phase concentration of adsorbate (mg/L) (initial concentration) K_L is the Langmuir constant (L/mg). The value of R_L indicates the shape of the isotherm accordingly as shown in Table 2. Adsorption system for a single, C_0 is usually the highest fluid-phase concentration encountered.

The value of the separation factor (R_L) for the present study is $0 < R_L < 1$ indicating that the shape of the isotherm is favorable [29]. Both Langmuir and Freundlich’s adsorption isotherm were found to fit the experimental data. The correlation coefficient (R^2) of Langmuir is slightly higher than that of Freundlich adsorption isotherm. These experimental studies on low-cost bio-adsorbent would be useful in

developing appropriate technology for the removal of heavy metals [22].

3.7. Kinetic Study. Figures 10(a)–10(e) showed the kinetics trends for Cu, Pb, Se, Zn, and Cr ion adsorption onto moringa (L and B), tea, sugarcane straw, and *Lupinus*. The relation between $\log (q_{eq} - q_t)$ and t was studied. The K_1 and q_e are obtained from the slope and intercept, respectively. The correlation coefficients (R^2) of the pseudo-first-order kinetic model are higher than the pseudo-second-order kinetic model, and q_e values calculated from the pseudo-first-order kinetic model are very close to the experimental ones. The results suggested that the overall rates of adsorption of Cu, Pb, Se, Zn, and Cr ions onto moringa (L, B), tea, sugarcane straw, and *Lupinus* are controlled by physical adsorption [45]. The theoretical q_{eq} values are equivalent to those observed for experimental q_{eq} values, suggesting that the bio-sorption followed a pseudofirst-order model.

TABLE 1: Parameters of models (Langmuir and Freundlich isotherm) for Cu, Se, Zn, Pb, and Cr adsorption on the moringa (L and B), tea, lupines, and sugarcane straw.

	Freundlich isotherm model					Langmuir isotherm model						
	Moringa M_L	Moringa M_B	Tea	Sugarcane straw	Lupines	Moringa M_L	Moringa M_B	Tea	Sugarcane straw	Lupines		
Pb	K_F	12.5	9.8	11.4	6.6	10	K_L	18.5	19	6.0	5.5	2.8
	n	4.2	4.2	3.0	4.4	2.6	q_m	14.5	11.4	15.0	8.9	16.1
	R^2	0.871	0.874	0.969	0.949	0.959	R^2	0.931	0.818	0.933	0.972	0.970
Cu	K_F	3.5	1.8	3.0	4.8	3.5	K_L	2.1	1.1	0.9	3.1	2.8
	n	3.3	2.0	2.3	3.6	3.6	q_m	5.7	4.3	5.8	7.1	5.7
	R^2	0.975	0.943	0.940	0.896	0.896	R^2	0.969	0.842	0.945	0.897	0.924
Cr	K_F	4.5	4.5	7.0	7.0	3.8	K_L	2.5	4.6	8.0	1.7	4.6
	n	4.3	4.0	3.9	3.0	6.5	q_m	6.8	5.6	8.8	12.7	4.9
	R^2	0.776	0.944	0.946	0.845	0.775	R^2	0.964	0.803	0.811	0.993	0.957
Zn	K_F	6.5	5.0	6	5	5	K_L	4.1	1.7	14.3	2.4	2.9
	n	4.0	3.1	7.8	3.5	3.53	q_m	9.3	8.1	7.1	6.8	6.9
	R^2	0.905	0.936	0.818	0.958	0.959	R^2	0.981	0.983	0.925	0.980	0.96
Se	K_F	3.5	3.9	3.9	2.8	3.8	K_L	1.0	1.2	4.1	1.7	5.3
	n	2.2	2.5	4.2	2.8	4.8	q_m	8.9	8.1	4.8	4.9	5.2
	R^2	0.977	0.965	0.984	0.984	0.966	R^2	0.988	0.991	0.833	0.927	0.841

TABLE 2: Characteristics of adsorption Langmuir isotherm.

Separation factor	Characteristics of adsorption Langmuir isotherm
$R_L > 1$	Unfavorable
$R_L = 1$	Linear
$0 < R_L < 1$	Favorable
$R_L = 0$	Irreversible

Besides, the value of R^2 (linear correlation) around 1 in pseudofirst-order confirms that the adsorption kinetics is controlled by this order and that there is a strong interaction between adsorbent and adsorbate. The pseudo-first-order kinetic suggests that physic-sorption is responsible for metal ions' adsorption.

Adsorption kinetic behavior of Cu, Se, Zn, Pb, and Cr adsorption on the moringa (L and B), tea, lupines, and sugarcane straw during the study I is presented in Table 3.

Table 4 shows the adsorption studies (Freundlich, Langmuir (F-L) model) for removing heavy metals in an aqueous solution using the different adsorbents.

3.8. Cost of Adsorbents. Based upon the preparation process used in this study, the cost analysis of using moringa, lupines, sugarcane straw, and tea as effective adsorbents of heavy metals from an aqueous solution was calculated as shown in Table 5. The cost analysis shows that the specific energy consumption of the adsorbent production is 3.5 kWh/m³ and water consumption is 0.035 m³. The cost

needed for the production of 0.1 kg of adsorbent is 3.535 Egyptian Pound, which is equivalent to \$0.177. This is considered a very low value as adsorbents produced from an agro waste at a priceless cost than other adsorbents such as activated carbon or other adsorbents [46]. Besides being a cost-effective treatment method for hazardous pollutants such as heavy metals, the adsorption process is environmentally friendly and does not generate secondary byproducts. The cost was calculated according to the following:

The cost for 0.1 kg of adsorbents = cost of materials + cost of electricity consumed. Hence, the cost = 0.035 + 3.5 = 3.535 L.E. for the production of 0.1 kg.

The adsorption study's overall results indicated the removal efficiency pattern as moringa > tea > *Lupinus* > sugarcane straw with corresponding maximum adsorption efficiency of 14.59, 16.10, 12.73, and 15.01 mg/g, respectively. Table 6 shows the adsorption efficiencies of some adsorbent-reported literature.

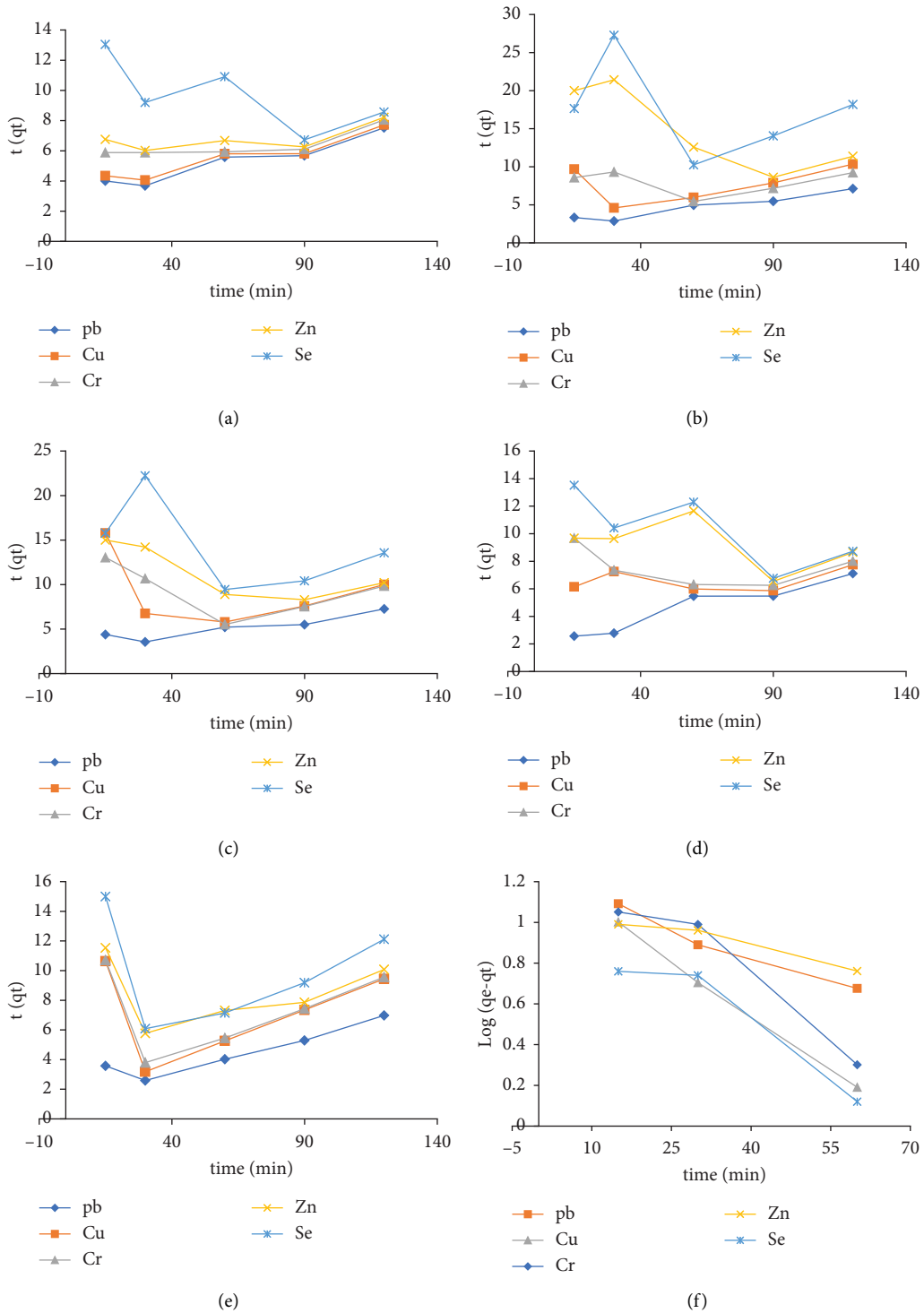


FIGURE 10: Continued.

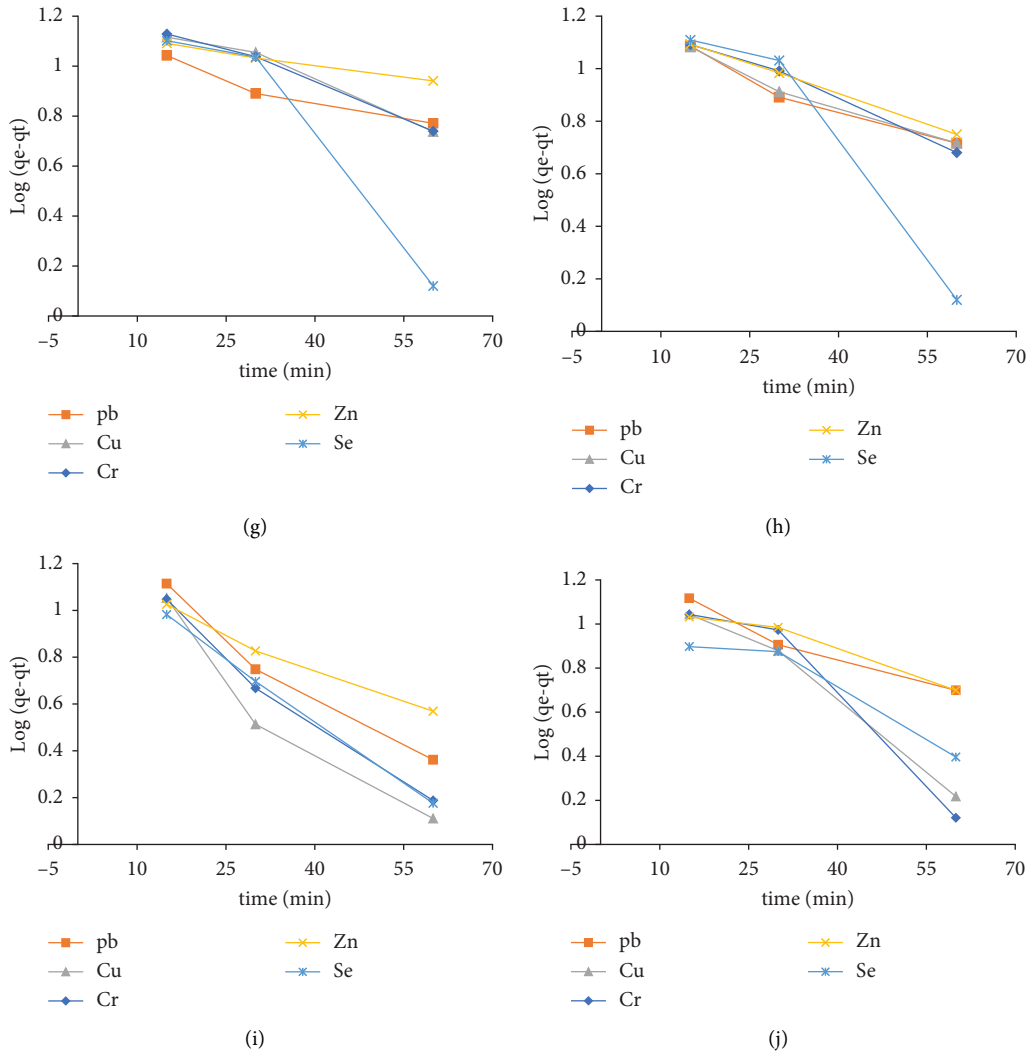


FIGURE 10: (a–e) The pseudo-first-order and pseudo-second-order of Pb, Cr, Se, Cu, and Zn onto moringa (L and B), tea, lupines, and sugarcane straw. (a) Pseudo first-order model of metals on SS. (b) Pseudo first-order model of metals on T. (c) Pseudo first-order model of metals on MB. (d) Pseudo first-order model of metals on L. (e) Pseudo first-order model of metals on ML. (f) Pseudo second-order model of metals on T. (g) Pseudo second-order model of metals on L. (h) Pseudo second-order model of metals on SS. (i) Pseudo second-order model of metals on ML. (j) Pseudo second-order model of metals on MB.

TABLE 3: The pseudo-first-order and the pseudo-second-order model parameters of Cu, Se, Zn, Pb, and Cr adsorption on the moringa (L and B), tea, lupines, and sugarcane straw.

Metals	Parameters	Pseudo-first-order model					Pseudo-second-order model					
		ML	MB	T	S	L	Parameters	ML	MB	T	S	L
Pb	K_1	0.017	0.008	0.008	0.007	0.005	K_2	0.001	0.001	0.001	0.001	0.001
	q_e	12.9	12.6	12.3	12.4	11	q_e	27.17	33.5	25.9	29.23	22.93
	R^2	0.999	0.962	0.970	0.976	0.933	R^2	0.8689	0.8425	0.9309	0.9072	0.921
Cu	K_1	0.019	0.018	0.017	0.007	0.008	K_2	0.001	0.001	0.001	0.001	0.001
	q_e	12.8	13.5	14.6	12.5	14	q_e	81.96	33.16	45.44	31.13	153.83
	R^2	0.927	0.980	0.997	0.975	0.989	R^2	0.0336	0.1052	0.163	0.8936	0.1
Cr	K_1	0.018	0.021	0.017	0.009	0.008	K_2	0.001	0.001	0.001	0.001	0.001
	q_e	12.69	15.3	14.9	13.5	14.1	q_e	69.93	31.9	476	58.82	72.99
	R^2	0.9849	0.9316	0.9337	0.9906	0.9882	R^2	0.0408	0.2148	0.003	0.638	0.1731
Zn	K_1	0.018	0.0077	0.0053	0.0076	0.0033	K_2	0.001	0.001	0.001	0.001	0.001
	q_e	12.69	12.8	11.2	13.2	12.4	q_e	2000	18.1	8.96	78.12	49
	R^2	0.9849	0.9599	0.955	0.9998	0.9957	R^2	0.003	0.5952	0.7301	0.4122	0.21
Se	K_1	0.0178	0.0118	0.0151	0.0232	0.0231	K_2	0.001	0.001	0.001	0.001	0.001
	q_e	12.89	12.9	11.2	33.2	32	q_e	357	15.8	20.4	25.25	21.2
	R^2	0.9994	0.9263	0.9087	0.9326	0.9269	R^2	0.002	0.2809	0.1107	0.5034	0.561

TABLE 4: The adsorption studies of removing heavy metals in aqueous solution using adsorbents Freundlich, Langmuir (F-L) model, kinetic model, adsorption capacity Q_{max} , contact time, dose, and initial concentration.

Metal	Adsorbent	pH	Dose (g)	Initial conc (mg/L)	Contact time (min)	Q_{max}	F-L models	Kinetic model	Type of metals solution
Pb	ML					25.4	L		
Cu						19.1	F		
Cr						9.7	L		
Zn						7.0	L		
Se						9.5	L		
Pb	MB					20.2	F		
Cu						8.0	F		
Cr						6.8	F		
Zn						5.5	L		
Se						1.4	L		
Pb	T	3.0-6.0-9.0	0.1-0.5	0.5-10	15-90	20.1	F	First-order model	Ternary
Cu						13	L		
Cr						7.0	F		
Zn						5.9	L		
Se						5.6	F		
Pb	S					9.8	L		
Cu						11.1	L		
Cr						8.5	L		
Zn						7.7	F		
Se						6.5	F		
Pb	L					22.7	L		
Cu						4.8	L		
Cr						7.0	L		
Zn						5.8	L		
Se						5.6	F		

TABLE 5: Material and energy consumption for production of 0.1 kg of adsorbents.

Process	Water consumption* (m ³)	Electricity consumption* (kWh)
Washing	0.002	—
Drying at 1050°C (24h)	—	2
Crushing and sieving	—	0.5
Washing	0.0015	—
Total consumption	0.0035	2.5
Cost	0.035	3.5

*In Egypt, the cost of 1 m³ of water for industrial use = 10.0 L.E. *In Egypt, the cost of 1 kWh of electricity for industrial use = 1.45 L.E.

TABLE 6: Adsorption efficiencies of some selected adsorbents.

Adsorbents	Adsorbents	Q_{max}	Reference
Untreated rice husk	Direct dyes	2.4	[47]
Activated rice husk	Direct dyes	4.3	[47]
Red-mud	Ni ⁺²	0.0018	[48]
Peanut hulls	Fe ⁺³ and Cu ⁺²	79.28 and 96.58 mg/g for Fe ⁺³ and Cu ⁺	[49]
Zeolite derived from fly ash	Cu ⁺²	14.7	[50]
Ag nanoparticle-loaded activated carbon (Ag-NP-AC)	Cu ⁺²	60	[51]
Iron oxide-coated eggshell powder	Cu ⁺²	6.7	[52]
Chitosan	Cu ⁺²	62.4	[53]

4. Conclusion

Nowadays, preventing water pollution due to the uncontrolled release of heavy metals is of vital need. Research is now focusing to develop a suitable technology either to prevent heavy metal pollution or to reduce it to a low level. Prevention of heavy metal to water bodies can be possible only by reducing their direct discharge into the water stream. The used conventional methods for removing heavy metals have many disadvantages such as high capital and operational cost, not suitable for small-scale industries, and inadequate efficiency. Adsorption is a promising process for heavy metals removal from wastewater. The process of adsorption is suitable at very low concentrations, i.e., 0.5 mg/L. Agrowaste materials are used as an adsorbent of heavy metals but the cost is a major draw of this adsorbent, thereby increasing the use of low-cost adsorbents for the treatment of wastewater. Agrowaste is a good option as it is a low-cost adsorbent for the removal of metals. Agrowaste is found to be an efficient adsorbent for metals like Se, Cr, Zn, Cu, and Pb. The experiment result shows the max. The removal of heavy metals (Se, Cr, Zn, Cu, and Pb) by agrowaste is 93%. In this research, moringa and other agrowaste seeds were investigated and their ability to aid metal removal was investigated. The results show that moringa leaves have a high removal percentage for heavy metals compared to other adsorbents, lupines, tea, and sugarcane straw. Moringa shows more than 90% of metal removal and the highest percentage of removal was achieved for Se, Cr, Zn, Cu, and Pb. The moringa leaves showed adsorption of metals for which the percentage adsorption for copper was about 76.6%, lead was about 90.2%, selenium was 70.5%, and chromium and zinc were about 76.5, and 78.9% which were higher compared to other adsorbents. The adsorption process occurred faster at pH 6.0. The obtained data of metal adsorption on the adsorbents were similar in both the models used, indicating the possible existence of more than one type of adsorption site interacting with the metal. The experimental data of metals adsorption on the adsorbents were fitted with the first-order model, indicating the adsorption occurs by the physical adsorption technique. Moringa can be considered an alternative for treating wastewater with toxic heavy metals such as copper, selenium, zinc, lead, and chromium, which is a low-cost option that requires no previous treatment.

Data Availability

The [Figures and Tables] data used to support the findings of this study are included within the article.

Conflicts of Interest

The authors declare that they have no conflicts of interest.

References

- [1] H. Abdel-Shafy and M. A. El-Khateeb, "Fate of heavy metals in selective vegetable plants irrigated with primary treated sewage water at slightly alkaline medium," *Egyptian Journal of Chemistry*, vol. 0, no. 0, p. 2312, 2019.
- [2] H. I. Abdel-Shafy, M. A. El-Khateeb, and M. Shehata, "Blackwater treatment via combination of sedimentation tank and hybrid wetlands for unrestricted reuse in Egypt," *Desalination and Water Treatment*, vol. 71, pp. 145–151, 2017.
- [3] H. I. Abdel-Shafy, M. A. Shoeib, M. A. El-Khateeb, A. O. Youssef, and O. M. Hafez, "Electrochemical treatment of industrial cooling tower blowdown water using magnesium-rod electrode," *Water resources and Industry*, vol. 23, Article ID 100121, 2020.
- [4] G. M. Geise, H. S. Lee, D. J. Miller, B. D. Freeman, J. E. McGrath, and D. R. Paul, "Water purification by membranes: the role of polymer science," *Journal of Polymer Science Part B: Polymer Physics*, vol. 48, no. 15, pp. 1685–1718, 2010.
- [5] M. Mokarram, A. Saber, and V. Sheykhi, "Effects of heavy metal contamination on river water quality due to release of industrial effluents," *Journal of Cleaner Production*, vol. 277, Article ID 123380, 2020.
- [6] M. Nandal, R. Hooda, and G. Dhanias, "Tea wastes as a sorbent for removal of heavy metals from wastewater," *Int. J. Curr. Eng. Technol*, vol. 4, no. 1, pp. 244–247, 2014.
- [7] W. Buah, J. MacCarthy, and S. Ndur, "Conversion of corn cobs waste into activated carbons for adsorption of heavy metals from minerals processing wastewater," *International Journal of Environmental Protection and Policy*, vol. 4, no. 4, pp. 98–103, 2016.
- [8] H. I. Abdel-Shafy and M. El-Khateeb, "Heavy metals in citrus fruits as affected by primary treated sewage irrigation," *Egyptian Journal of Chemistry*, vol. 64, no. 1, pp. 165–176, 2021.
- [9] Y. Luo, "Study on the repair of heavy metal contaminated soil," in *IOP Conference Series: Earth and Environmental Science* IOP Publishing, Bristol, England, UK, 2019.
- [10] N. Jean Claude, L. Shanshan, J. Khan, W. Yifeng, H. dongxu, and L. Xiangru, "Waste tea residue adsorption coupled with electrocoagulation for improvement of copper and nickel ions removal from simulated wastewater," *Scientific Reports*, vol. 12, no. 1, pp. 3519–3618, 2022.
- [11] J. Mofeed, "Biosorption of heavy metals from aqueous industrial effluent by non-living biomass of two marine green algae *Ulva lactuca* and *Dunaliella salina* as Biosorbents," *Catrina: International Journal of Environmental Sciences*, vol. 16, no. 1, pp. 43–52, 2017.
- [12] V. Nand, "Water purification using moringa oleifera and other locally available seeds in Fiji for heavy metal removal," *International Journal of Applied*, vol. 2, no. 5, pp. 125–129, 2012.
- [13] R. Shrestha, S. Ban, S. Devkota et al., "Technological trends in heavy metals removal from industrial wastewater: a review," *Journal of Environmental Chemical Engineering*, vol. 9, no. 4, Article ID 105688, 2021.
- [14] L. M. Plum, L. Rink, and H. Haase, "The essential toxin: impact of zinc on human health," *International Journal of Environmental Research and Public Health*, vol. 7, no. 4, pp. 1342–1365, 2010.
- [15] J. A. Cotruvo, "2017 WHO guidelines for drinking water quality: first addendum to the fourth edition," *Journal*

- American Water Works Association*, vol. 109, no. 7, pp. 44–51, 2017.
- [16] H. I. Abdel-Shafy, "Removal of Cadmium, Nickel, and Zinc from aqueous solutions by activated carbon prepared from corn-cob-waste agricultural materials," *Egyptian Journal of Chemistry*, vol. 65, no. 3, pp. 1-2, 2022.
- [17] S. J. Fairweather-Tait, Y. Bao, M. R. Broadley et al., "Selenium in human health and disease," *Antioxidants and Redox Signaling*, vol. 14, no. 7, pp. 1337–1383, 2011.
- [18] S. Shahabuddin, N. Muhamad Sarih, S. Mohamad, and J. Joon Ching, "SrTiO₃ nanocube-doped polyaniline nanocomposites with enhanced photocatalytic degradation of methylene blue under visible light," *Polymers*, vol. 8, no. 2, p. 27, 2016.
- [19] S. Shahabuddin, N. M. Sarih, S. Mohamad, and S. N. Atika Baharin, "Synthesis and characterization of Co₃O₄ nanocube-doped polyaniline nanocomposites with enhanced methyl orange adsorption from aqueous solution," *RSC Advances*, vol. 6, no. 49, pp. 43388–43400, 2016.
- [20] S. Shahabuddin, R. Khanam, M. Khalid et al., "Synthesis of 2D boron nitride doped polyaniline hybrid nanocomposites for photocatalytic degradation of carcinogenic dyes from aqueous solution," *Arabian Journal of Chemistry*, vol. 11, no. 6, pp. 1000–1016, 2018.
- [21] S. Shahabuddin, N. M. Sarih, F. H. Ismail, M. M. Shahid, and N. M. Huang, "Synthesis of chitosan grafted-polyaniline/Co₃O₄ nanocube nanocomposites and their photocatalytic activity toward methylene blue dye degradation," *RSC Advances*, vol. 5, no. 102, pp. 83857–83867, 2015.
- [22] V. C. Gonçalves dos Santos, C. A. de Toledo Gomes, D. Cardoso Dragunski, L. A. Deitos Koslowski, and K. Lunelli, "Removal of metals ions from aqueous solution using modified sugarcane bagasse," *Revista Virtual de Química*, vol. 11, no. 4, pp. 1289–1301, 2019.
- [23] H. Ahmed, M. El-Khateeb, and N. ahmed, "Effective granular activated carbon for greywater treatment prepared from corn-cobs," *Egyptian Journal of Chemistry*, vol. 10, Article ID 117621, 2022.
- [24] P. S. Kumar and K. Kirthika, "Equilibrium and kinetic study of adsorption of nickel from aqueous solution onto bael tree leaf powder," *Journal of Engineering Science and Technology*, vol. 4, no. 4, pp. 351–363, 2009.
- [25] Apha, *Standard Methods for Examination of Water and Wastewater*, American Public Health Association, Washington, D.C, USA, 2021.
- [26] F. Sadon, A. S. Ibrahim, and K. N. Ismail, "An overview of rice husk applications and modification techniques in wastewater treatment," *J Purity Utility Reaction Environ*, vol. 1, pp. 308–334, 2012.
- [27] S. Obeng Apori, "Moringa oleifera seeds as a low-cost biosorbent for removing heavy metals from waste water," 2020, https://www.researchgate.net/publication/341827366_MORINGA_OLEIFERA_SEEDS_AS_A_LOW-COST_BIOSORBENT_FOR_REMOVING_HEAVY_METALS_FROM_WASTEWATER.
- [28] M. A. Mahmoud, "Thermodynamics and kinetics studies of Mn (II) removal from aqueous solution onto powder corn cobs (PCC)," *Journal of Chromatography and Separation Techniques*, vol. 06, no. 07, p. 1, 2015.
- [29] M. N. E. Alam, M. A. S. Mia, and M. Chowdhury, "BOD reduction using spent tea waste from Tannery wastewater," *J Sci Innov Res*, vol. 6, no. 2, pp. 58–62, 2017.
- [30] C. Arunkumar, "Use of corn cob as low cost adsorbent for the removal of nickel (II) from aqueous solution," *International Journal of Advanced Biotechnology and Research*, vol. 5, pp. 325–330, 2014.
- [31] K. Shruthi and M. Pavithra, "A study on utilization of groundnut shell as biosorbent for heavy metals removal," *International Journal of Engineering and Technology*, vol. 4, no. 3, pp. 411–415, 2018.
- [32] M. Ghasemi, N. Ghasemi, G. Zahedi, S. R. W. Alwi, M. Goodarzi, and H. Javadian, "Kinetic and equilibrium study of Ni (II) sorption from aqueous solutions onto Peganum harmala-L," *International journal of Environmental Science and Technology*, vol. 11, no. 7, pp. 1835–1844, 2014.
- [33] I. Nhapi, "Removal of heavy metals from industrial wastewater using rice husks," *The Open Environmental Engineering Journal*, vol. 4, no. 1, pp. 170–180, 2011.
- [34] I. W. Maina, V. Obuseng, and F. Nareetsile, "Use of Moringa oleifera (Moringa) seed pods and Sclerocarya birrea (Morula) nut shells for removal of heavy metals from wastewater and borehole water," *Journal of Chemistry*, vol. 2016, Article ID 9312952, 13 pages, 2016.
- [35] A. K. Nasim, I. Shaliza, and S. Piarapakaran, "Elimination of heavy metals from wastewater using agricultural wastes as adsorbents," *Malaysian Journal of Science*, vol. 23, no. 1, pp. 43–51, 2004.
- [36] H. de Fátima Gorgulho, V. V. da Silva Guilharduci, and P. B. Martelli, *Sugarcane Bagasse As Potentially Low-Cost Biosorbent*, Sugarcane technology and research, Tamil Nadu, India, 2018.
- [37] K. H. Vardhan, P. S. Kumar, and R. C. Panda, "A review on heavy metal pollution, toxicity and remedial measures: current trends and future perspectives," *Journal of Molecular Liquids*, vol. 290, Article ID 111197, 2019.
- [38] V. C. G. Dos Santos, J. V. T. M. De Souza, C. R. T. Tarley, J. Caetano, and D. C. Dragunski, "Copper ions adsorption from aqueous medium using the biosorbent sugarcane bagasse in natura and chemically modified," *Water, Air, and Soil Pollution*, vol. 216, no. 1-4, pp. 351–359, 2011.
- [39] I. Ghorbel-Abid and M. Trabelsi-Ayadi, "Competitive adsorption of heavy metals on local landfill clay," *Arabian Journal of Chemistry*, vol. 8, no. 1, pp. 25–31, 2015.
- [40] P. Ximénez-Embún, Y. Madrid-Albarran, C. Camara, C. Cuadrado, C. Burbano, and M. Muzquiz, "Evaluation of lupinus species to accumulate heavy metals from W aste waters," *International Journal of Phytoremediation*, vol. 3, no. 4, pp. 369–379, 2001.
- [41] A. Waheed, R. Sabir, and A. Salahuddin, "Comparative study on raw and modified forms of sugarcane bagasse for biosorption of Cu from wastewater," 2022, https://www.researchgate.net/publication/350631755_Comparative_study_on_raw_and_modified_forms_of_sugarcane_bagasse_for_biosorption_of_Cu_2_from_wastewater.
- [42] E. N. Ali and H. T. Seng, "Heavy metals (Fe, Cu, and Cr) removal from wastewater by Moringa oleifera press cake," in *MATEC Web of Conferences*EDP Sciences, Cedex, France, 2018.
- [43] P. L. Homagai, K. N. Ghimire, and K. Inoue, "Adsorption behavior of heavy metals onto chemically modified sugarcane bagasse," *Bioresource Technology*, vol. 101, no. 6, pp. 2067–2069, 2010.
- [44] A. C. Gonçalves Junior, A. P. Meneghel, F. Rubio, L. Strey, D. C. Dragunski, and G. F. Coelho, "Applicability of Moringa oleifera Lam. pie as an adsorbent for removal of heavy metals from waters," *Revista Brasileira de Engenharia Agrícola e Ambiental*, vol. 17, no. 1, pp. 94–99, 2013.

- [45] M. E. A. A. Ibrahim Hegazy, E. H. Zaghlool, and R. Elsheikh, "Review Article: heavy metals adsorption from contaminated water using moringa seeds/olive pomace byproducts," *Applied Water Science*, vol. 95, pp. 5–14, 2021.
- [46] A. S. Sayed, M. Abdelmottaleb, M. F. Cheira, G. Abdel-Aziz, H. Gomaa, and T. F. Hassanein, "Date seed as an efficient, eco-friendly, and cost-effective bio-adsorbent for removal of thorium ions from acidic solutions," *Aswan University Journal of Environmental Studies*, vol. 1, no. 1, pp. 106–124, 2020.
- [47] O. Abdelwahab, "Use of rice husk for adsorption of direct dyes from aqueous solution: a case study of Direct F. Scarlet," *Egyptian Journal of Aquatic Research*, vol. 31, no. 1, pp. 1–11, 2005.
- [48] S. Lakshmi Narayan, V. Govindan, and C. Arunkumar, "A batch studies on adsorption of Nickel (II) using redmud," *International Journal of Advanced Research*, vol. 1, no. 9, pp. 465–472, 2013.
- [49] O. E. Abdel Salam, N. A. Reiad, and M. M. ElShafei, "A study of the removal characteristics of heavy metals from wastewater by low-cost adsorbents," *Journal of Advanced Research*, vol. 2, no. 4, pp. 297–303, 2011.
- [50] T. Mishra and S. Tiwari, "Studies on sorption properties of zeolite derived from Indian fly ash," *Journal of Hazardous Materials*, vol. 137, no. 1, pp. 299–303, 2006.
- [51] S. Shahmirifard, M. Ghaedi, M. Rahimi, S. Hajati, M. Montazerzohori, and M. Soylak, "Simultaneous extraction and preconcentration of Cu^{2+} , Ni^{2+} and Zn^{2+} ions using Ag nanoparticle-loaded activated carbon: response surface methodology," *Advanced Powder Technology*, vol. 27, no. 2, pp. 426–435, 2016.
- [52] Y. Liu, P. Liang, and L. Guo, "Nanometer titanium dioxide immobilized on silica gel as sorbent for preconcentration of metal ions prior to their determination by inductively coupled plasma atomic emission spectrometry," *Talanta*, vol. 68, no. 1, pp. 25–30, 2005.
- [53] G. Crini, "Recent developments in polysaccharide-based materials used as adsorbents in wastewater treatment," *Progress in Polymer Science*, vol. 30, no. 1, pp. 38–70, 2005.